THEORETICAL ANALYSIS OF A RIDGED-WAVEGUIDE MOUNTING STRUCTURE

S. Mizushina, N. Kuwabara, H. Kondoh
The Research Institute of Electronics
Shizuoka University
Hamamatsu 432, Japan

Abstract

The driving-point impedance of a single-gap thin conductor strip, a model of the ribbon-and-pedestal of device package, mounted across the gap of a ridged waveguide has been derived using the induced EMF method. The dyadic Green's function for the ridged waveguide was derived to facilitate the analysis. An equivalent circuit was developed which involved an infinite array of transformers representing the couplings between the conductor strip and the waveguide normal modes. Numerical results for a typical example were also given, demonstrating a remarkably smooth behavior of the driving-point impedance of the mount over a frequency range from 5.4 GHz to 25.4 GHz.

Introduction

Ridged waveguides have been used for many years in microwave components and systems requiring wide bandwidths. Among such applications mounting structures for solid-state devices are of our interest here[1,2]. A recent experimental investigation showed that mechanical tuning ranges of 8.5-26 GHz and 14-28 GHz were achieved with Gunn and IMPATT diodes, respectively, mounted in the ridged-waveguide cavity[3,4]. This urged us to study the ridged-waveguide mounting structure theoretically as well. The analysis presented in this paper is an extension of the induced EMF method previously developed for the rectangular waveguide mounting structures[5,6]. The mounting structure considered here is illustrated in Fig.1(a), where the packaged diode fits in the gap between the ridges extending uniformly to infinity in the z direction. Neglecting the ceramic ring and replacing the ribbon-and-pedestal of the package by a single-gap thin conductor strip, as shown in Fig.1(b), we can derive the driving-point impedance of the mount.

Analysis

We regard the thin conductor strip with a width w and a gap g as a small antenna radiating into the ridged waveguide. Since w is small, the current in the conductor strip can be represented by

$$\bar{J}(\bar{R}) = \begin{cases} \hat{y} J_o \sum_{n=o}^{\infty} A_n \cos\frac{n\pi}{b_3}(y-b_3)\,\delta(z-0), & -\frac{w}{2} \le x \le \frac{w}{2} \\ 0, & \text{otherwise} \end{cases} \tag{1}$$

where $\hat{y}$ is the y-directed unit vector. This current excites fields which may be represented by an infinite sum of the waveguide normal modes. The complete eigenvalue solution of ridged waveguide needed here has been obtained by Montgomery[7]. Quoting from his result, we can write for the y component of the electric basis field in the region 1, referring to Fig.1, as

$$e_{Hy}(\bar{R}) = -\sum_{n=o}^{\infty} \eta_{1n} k_{x1n} \cos k_{x1n} x \cos\frac{n\pi}{b_3}(y-b_3) \tag{2}$$

for TE modes and

$$e_{Ey}(\bar{R}) = \sum_{n=1}^{\infty} \xi_{1n} \frac{n\pi}{b_3} \cos k_{x1n} x \cos\frac{n\pi}{b_3}(y-b_3) \tag{3}$$

for TM modes, where k_{x1n} is defined by

$$k_{x1n} = \begin{cases} \sqrt{k_T^2 - (\frac{n\pi}{b_3})^2}, & k_T \ge \frac{n\pi}{b_3} \\ -j\sqrt{(\frac{n\pi}{b_3})^2 - k_T^2}, & k_T < \frac{n\pi}{b_3} \end{cases} \tag{4}$$

In equ.(4) k_T is an eigenvalue and k_{x1n} is the propagation constant in the x direction of spatial harmonic components in the region 1 associated with the eigenvalue. The amplitudes of these spatial harmonic components are η_{1n} and ξ_{1n} in equs.(2) and (3) and are determined from the normalization condition by the method described in Ref.7. We retain in this analysis only those modes which satisfy the magnetic-wall-boundary condition at the symmetry plane since the current strip is at the center of the waveguide.

With the complete eigenvalue solution in our hand, we can derive the dyadic Green's function for the ridged waveguide using Tai's procedure[8]. The $\hat{y}\hat{y}$ component of the Green's function may be presented in the form

$$\begin{aligned} -G_{yy}(\bar{R}) = {} & j\sum_{k_{TH}} \sum_{n=o}^{\infty} \frac{\exp(-j\Gamma_H|z-z'|)}{2\Gamma_H} (\eta_{1n} k_{x1n})^2 \\ & \cdot \cos k_{x1n} x \cos k_{x1n} x' \cos\frac{n\pi}{b_3}(y-b_3)\cos\frac{n\pi}{b_3}(y'-b_3) \\ & + j\sum_{k_{TE}} \sum_{n=1}^{\infty} \frac{\Gamma_E \exp(-j\Gamma_E|z-z'|)}{2k^2} (\xi_{1n}\frac{n\pi}{b_3})^2 \\ & \cdot \cos k_{x1n} x \cos k_{x1n} x' \cos\frac{n\pi}{b_3}(y-b_3)\cos\frac{n\pi}{b_3}(y'-b_3) \end{aligned} \tag{5}$$

where k_{TH} and k_{TE} are the eigenvalues, Γ_H and Γ_E are the propagation constants of the TE and TM modes, respectively, and $k^2=\omega^2\varepsilon_o\mu_o$.

Substituting equs.(1) and (5) into

$$E_y(\bar{R}) = -j\omega\mu_o \int_{vol} G_{yy}(\bar{R}/\bar{R}')J(\bar{R}')dv' \tag{6}$$

we obtain the electric field excited by the current in the conductor strip.

For a gap with small w and g, we can assume a uniform voltage, V, across the gap, so that the gap field is given by

$$\bar{E}_{gap}(\bar{R}) = -\hat{y}\,\frac{V}{g}\,v(x)v(y)v(z) \tag{7}$$

$$v(x) = \begin{cases} 1, & -\frac{w}{2} \le x \le \frac{w}{2} \\ \text{arbitrary}, & \text{otherwise} \end{cases}$$

$$v(y) = \begin{cases} 1, & h - \frac{g}{2} \le y \le h + \frac{g}{2} \\ 0, & \text{along the conductor strip} \end{cases}$$

$$v(z) = \begin{cases} 1, & z = 0 \\ \text{arbitrary}, & z \neq 0 \end{cases}$$

Applying the Lorentz reciprocity theorem to $\bar{J}(\bar{R})$, $\bar{E}(\bar{R})$, and $\bar{E}_{gap}$, we have

$$\int_{vol} J_y E_{gap}\,dv = \int_{vol} J_y E_y\,dv \tag{8}$$

From equ.(8) we can derive the driving-point impedance, Z_R, seen at the gap terminals using the procedure described by Eisenhart and Khan[6].

Results are:

$$\frac{1}{Z_R} = \sum_{n=o}^{\infty} \frac{1}{Z_n} \tag{9}$$

$$Z_n = \frac{1}{K_{gn}^2}\left[\sum_{THp} k_{THp} K_{sHnp}^2 \frac{\omega\mu_o}{\Gamma_{Hp}} + \sum_{TEq} k_{TEq} K_{sEnq}^2 \frac{\Gamma_{Eq}}{\omega\varepsilon_o}\right] \tag{10}$$

where

$$K_{gn} = \sqrt{2}\left[\frac{2}{b_3(1+\delta_o)}\right]\cos\frac{n\pi}{b_3}(h-b_3)\left(\frac{\sin\phi_n}{\phi_n}\right) \tag{11}$$

$$\delta_o = \begin{cases} 1, & n = 0 \\ 0, & n \neq 0 \end{cases}$$

with $\phi_n = \frac{n\pi}{b_3}\frac{g}{2}$ and

$$K_{sHnp} = \eta_{1n}\, k_{x1n}\left(\frac{\sin\theta_n}{\theta_n}\right) \tag{12}$$

$$K_{sEnq} = \xi_{1n}\,\frac{n\pi}{b_3}\left(\frac{\sin\theta_n}{\theta_n}\right) \tag{13}$$

with $\theta_n = k_{x1n}\frac{w}{2}$.

The factor K_{gn} is the gap coupling factor. Similarly, K_{sHnp} and K_{sEnq} are the conductor-strip coupling factor for the TE and TM modes, respectively.

Equations (10) through (13) can readily be represented by an equivalent circuit as shown in Fig.2. The parallel connection of Z_n as shown in Fig.3 gives the driving-point impedance, Z_R, in view of equ.(9). In practice the frequency of operation is restricted so that only the dominant TE_{10}-hybrid mode propagates while all other higher-order modes evanesce. Then, Z_{H1} is resistive, Z_{Hp} ($p \ge 2$) inductive, Z_{Eq} ($q \ge 1$) capacitive. For $n \ge 1$, the net effect of Z_{Hp} and Z_{Eq} is capacitive. In addition, $K_{sHn1} \simeq 0$ owing to small values of η_{1n} for the dominant mode. Hence, the equivalent circuit of Fig.3 reduces to the simple one shown in Fig.4, where $Z_{c10}/2 = (K_{sH01}/K_{g0})^2(\omega\mu_o/\Gamma_{H1})$.[7]

Results of numerical computation for w=1.00, g=0.50, h=0.90, a_1=1.75, a_2=7.90, b_1=4.85, b_2=3.05, b_3=1.80 (all are given in millimeters) are presented in Fig.5. The solid and the broken curves represent the real and the imaginary parts, respectively, of Z_R (= $R_R + jX_R$) obtained by equ.(9). The results demonstrate a remarkably smooth behavior of Z_R over a very wide frequency range, which is bounded by the higher-order-mode resonances at about the cut-off frequencies of TE_{10}-hybrid (5.4 GHz) and TE_{30}-hybrid modes (25.4 GHz). The crosses and circles in Fig.5 represent the real and the imaginary parts of Z_R' (= $R_R' + jX_R'$) obtained from Fig.4, where Z_{c10} is the characteristic impedance of the dominant mode. Comparison between Z_R and Z_R' gives a justification for the use of the simplified equivalent circuit in practical designs and analyses of microwave circuits.

As the width of the strip decreases, the number of eigenvalues required for computation increases. Fig.6 is the plot of inductance, L, versus the strip width, w, evaluated at 10 GHz for the previously cited dimensions using a different number of eigenvalues. For w=1.00 mm, eigenvalues up to 300 GHz were required, giving L=0.90 nH and C=0.03 pF (g=0.50 mm) with $n \le 4$.

Conclusions

A ridged-waveguide mounting structure has been analysed theoretically. The ribbon-and-pedestal of microwave diode package was replaced by a thin conductor strip with a gap, which was regarded as a small antenna radiating into the waveguide. The driving-point impedance was derived using the induced EMF method with the aid of the dyadic Green's function for the ridged waveguide which was also derived and presented. Results of the analysis was put in the form of equivalent circuit showing the couplings of the conductor strip to the waveguide normal modes. The equivalent circuit was then reduced to a simple one convenient for use in practical designs and analyses of microwave circuits. Numerical results obtained for a typical example were also given, demonstrating a remarkably smooth behavior of the driving-point impedance of the mount over a frequency range from 5.4 to 25.4 GHz.

Neglection of the package ceramic ring is a major limitation. However, the results presented in this paper will be useful for designs and analyses of various broad-band microwave components involving small devices as well as for characterization of these devices.

References

1. D. H. Claxton and P. T. Greiling, "Broad-Band Varactor-tuned IMPATT-Diode Oscillator," IEEE Trans., MTT-23, pp.501-504, June 1975.

2. P. J. Meier, "Integrated Fin-Line Millimeter Components," IEEE Trans., MTT-22, pp.1209-1216, Dec. 1974.

3. S. Mizushina and T. Ohsuka, "The Ridged-Waveguide-Cavity Gunn Oscillator for Wideband Tuning," IEEE Trans., MTT-24, pp.257-259, May 1976.

4. H. Kondoh, S. Mizushina and N. Kuwabara, "Broad-Band IMPATT and Gunn Oscillators with Ridged-Waveguide Cavity," IECEJ Tech. Rept., MW-76-130, January 1977.

5. E. Yamashita and J. R. Baird, "Theory of Tunnel Diode Oscillator in a Microwave Structure," Proc. IEEE, vol.54, pp.606-611, April 1966.

6. R. L. Eisenhart and P. J. Khan,"Theoretical and Experimental Analysis of a Waveguide Mounting Structure," IEEE Trans., MTT-19, pp.706-719, August 1971.

7. J. P. Montgomery, "On the Complete Eigenvalue Solution of Ridged Waveguide," IEEE Trans., MTT-19, pp.547-555, June 1971.

8. C. T. Tai, Dyadic Green's Functions in Electromagnetic Theory, Scranton: Intext Educational Publ., 1971, pp.69-80.

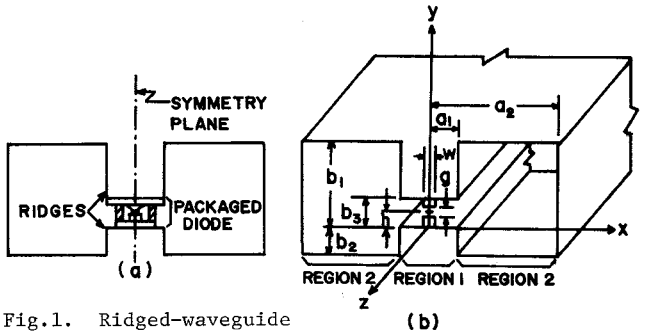

Fig.1. Ridged-waveguide mounting structure.
(a) Cross section of an actual mount.
(b) Model used in the analysis.

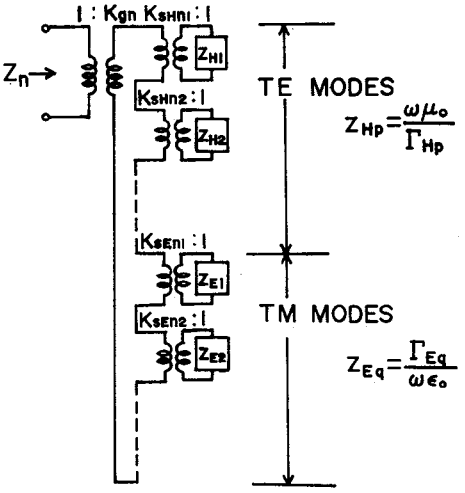

Fig.2. An equivalent circuit of Z_n.

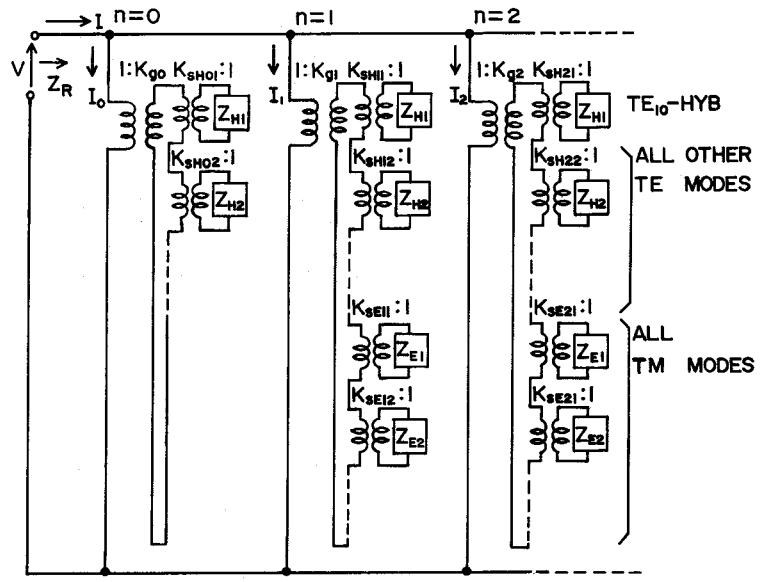

Fig.3. An equivalent circuit of the driving-point impedance of the ridged-waveguide mount.

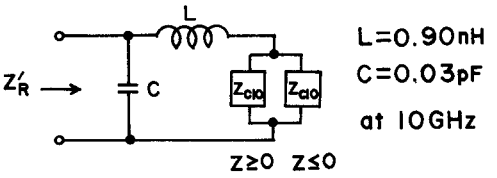

Fig.4. A simplified equivalent circuit.

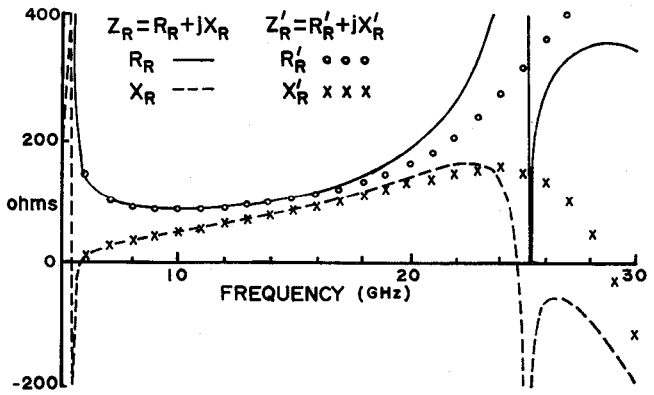

Fig.5. Frequency characteristics of the real and imaginary parts of Z_R and Z_R'.

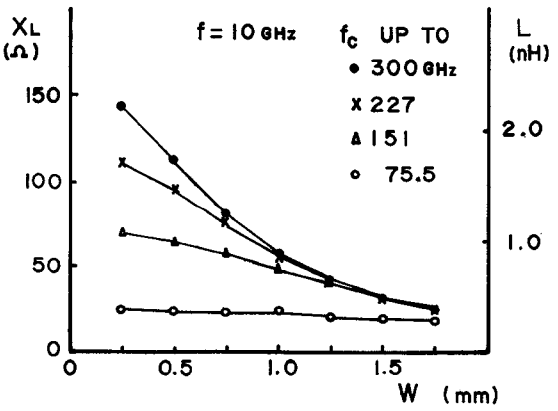

Fig.6. Inductance versus strip width. Inductance is evaluated with a different number of eigenvalues.